

Hydrochemistry and Groundwater Quality Assessment along Wadi Al-Showat, Khamis Mushayt District, South-West Saudi Arabia

¹Alfaiifi, ^{1,2}H.J. Albassam, ¹A.M. Kahal, ¹A.Y. Ibrahim, ^{1,3}E.H. Kamal Abdel Rahman,
¹Faisal K. Zaidi, ¹SM. Alhumidan, ¹Nassir S. Alarifi and ⁴Oumar Loni

¹Department of Geology and Geophysics, King Saud University, Riyadh, Saudi Arabia
²SGS Research Chair

³Department of Seismology, National Research Institute of Astronomy and Geophysics, Cairo, Egypt
⁴King Abdul-Aziz City for Science and Technology, Riyadh, Saudi Arabia

Abstract: Along Wadi Al Showat, fractured/weathered basement rocks serve as the local aquifer and store significant quantities of water to fulfil the domestic and agricultural demands of the local population. Twenty seven groundwater samples were collected from shallow dug wells and hydrochemically analysed. Although the average TDS value (792.67 mg/l) is not very high, the ionic relationship plots point towards anthropogenic sources of pollution. The water in the area belongs to the SO₄-Cl type of facies. Despite the fractured nature of the aquifer, therefore and the occurrence of water table at shallow depths, the water appears to be relatively unpolluted.

Key words: Hydrochemistry • Groundwater • Quality • Assessment • Saudi Arabia

INTRODUCTION

The western part of Saudi Arabia, geologically referred to as the Arabian Shield, extends from the Gulf of Aqaba to the Gulf of Aden and is dominated by crystalline rocks that are characterized by very low primary porosity and permeability. This area, therefore, has limited groundwater reserves, with those that do exist being stored mostly in the alluvial deposits along the wadi channels or the weathered/fractured/jointed basement rocks [1]. The source of this limited available groundwater supply depends on the orographic rainfall received along the western, southwestern and south-eastern mountain ridges of the Arabian Shield [2]. The limited availability of water in these regions due to the semiarid or arid climates and the presence of basement rocks restrict the availability of groundwater. Nevertheless, these basement rocks can in some circumstances serve as shallow aquifers thanks to the development of secondary porosity in the form of fissures and fractures, which can be derived from cooling stresses in the magma, subsequent tectonic activity [3], or lithostatic decompression processes [4, 5, 6]. Recent work demonstrates that these

secondary porosities can also be a result of the geomorphological processes of deep weathering and erosion [7, 8, 9].

In these fractured rocks, groundwater flows only through conduits and the aquifer matrix between the conduits is impermeable and has no porosity [10]. These weathered and fractured rocks can be an important source of groundwater and can form reliable aquifers in many arid areas [11, 12]. The ability of fractures to act as conduits for groundwater flow is affected by the degree to which the fractures are interconnected. Fracture connectivity increases with increasing fracture length and fracture density.

One of the vital factors in assessing the amount of water available to meet the various demands of agriculture, industry and other human activities is the amount of rainfall. The desert climate is dominant in Saudi Arabia, with very hot summers all over the country and rain very scarce almost everywhere. The south-western region of Saudi Arabia is located within the subtropical climate zone and receives a higher amount of rainfall in comparison to other regions, since it is mountainous with elevations reaching more than 2000 m (a.m.s.l).

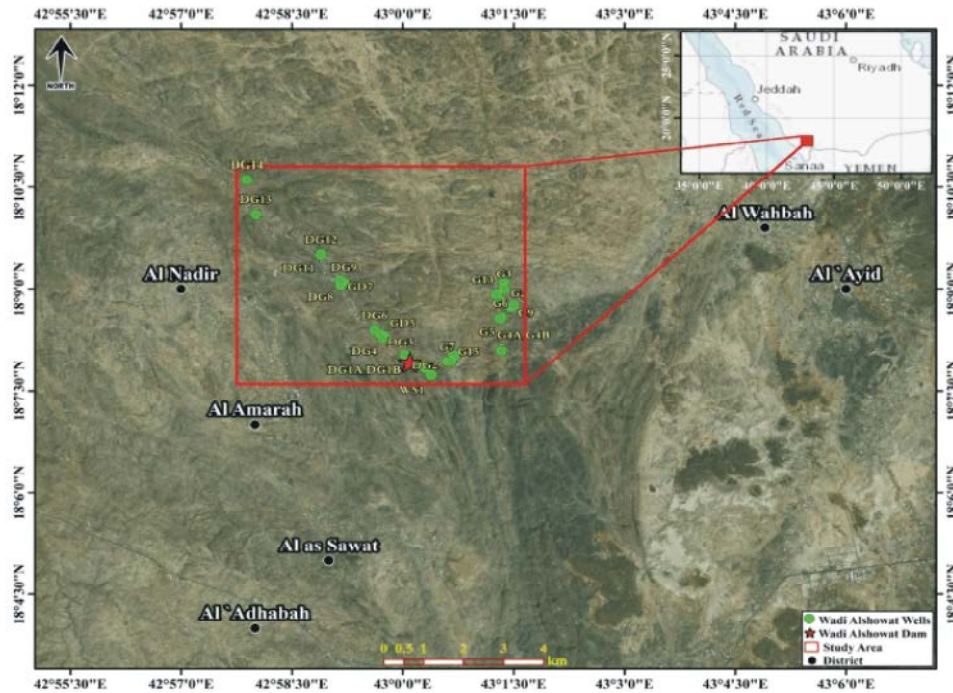


Fig. 1: Location map for Wadi Al-Showat area

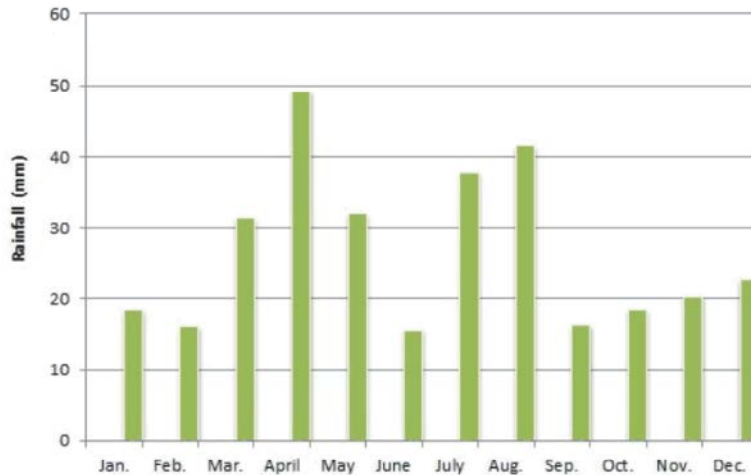


Fig. 2: The monthly average rainfall of Wadi Al-Showat area

These highlands receive variable rainfall in winter caused by westerly depressions and in summer caused by the south-western monsoon, which brings damp oceanic winds, clouds and fog [13]. The study area lies within the south-western zone (Figure 1) and the average annual rainfall can reach more than 300 mm (Figure 2) [14].

Wadi Al-Showat is characterized by increasing population and agricultural activities (Figure 3a and 3b). The inhabitants discharge their sewage waste directly into the ground through sewage pipes, as shown in Figure

3a. Fortunately, the total human population and the number of these rural houses are still limited. In addition, there is agricultural activity along the course of the wadi. These two activities (uncontrolled sewage disposal and agricultural return flow) make the shallow aquifer in the area vulnerable to pollution. Regular monitoring of groundwater quality is therefore required in the area to study the nature and extent of pollution. The main purpose of the present study was to assess the groundwater chemistry using hydrochemical analysis integrated with geological field investigation.



Fig. 3: Field photos showing the urban and agricultural hazardous activities along Wadi Al-Showat area

Description of the Study Area

Physiography and Geological Setting: The study area lies about 30 km to the south west of Khamis Mushayt and has an elevation of more than 2000m above mean sea level and is a part of the Sarwat Mountains of western Saudi Arabia. The area receives less than 400 mm of rain annually and the typical summer temperatures are 20-25°C and around 10°C in winter, with occasional snowfall along higher elevations (Miller 1994). There is a dam present in the study area.

The study area is underlain predominantly by the upper Proterozoic metamorphosed volcanic and sedimentary rocks of the Bahah and Jeddah groups and by upper Proterozoic plutonic rocks ranging in composition from gabbro to granite [15]. The Jeddah group consists of local, thick, deposits of basalt andesite and dacite. The Bahah group is present as biotite-quartz schist, carbonaceous phyllite and subordinate calcareous phyllite containing marble beds. In addition, Tertiary and Quaternary basalt and Quaternary surficial deposits overlie the Proterozoic rocks. The area of study is affected by north-trending faults or fault zones which are superimposed on the volcanic-arc complexes and Proterozoic intrusive rocks (Figure 4).

The study area is covered with fractured and jointed diorite, granodiorite and granitic rocks that are intruded with alkali-feldspar granite and pegmatite (Figure 5). Fractures with west-northwest to north-west and east to west trends are observed in the field. These fracture zones date from the Tertiary period and are related to the Red Sea rifting, or were reactivated during the Phanerozoic [16]. In some places, the granitic rocks are intruded by

coarse-grained, quartz-rich quartzite grained monzogranite and pegmatite veins that have a coarse-grained weathering product and they therefore tend to develop and preserve open joint systems between the granitic blocks. These fracturing systems are important from a hydrogeological point of view since they facilitate the storage and flow of water through them and also facilitate the vertical infiltration of the surface pollutants.

Hydrogeology and Basin Morphometry: Depth to groundwater levels were taken from 27 observation wells in July, 2015. All the observation wells fall within the north-western part of the basin. The piezometric map (Figure 6) shows a general groundwater flow direction from east to west. Extrapolation of piezometric levels in the southern part of the basin has been avoided due to the absence of water level data. The maximum and minimum piezometric level ranges from 2143.07 to 2204.35 metres above mean sea level.

The Wadi Al Showat basin (Figure 7) was delineated from the ASTER Global Digital Elevation Map using the hydrological processing tool in ArcGIS. The basin covers an area of approximately 92.86 km². As shown by the stream distribution in the map of the study area, the basin is a 5th order basin with most of the water sample locations falling along the main 5th order basin. The maximum and minimum elevation in the basin ranges from 2432 metres to 2130 metres, with an average elevation of 2274 metres above mean sea level. The streamflow is from a southeast to northwest direction. In general the streams flow in a dendritic pattern, which is influenced by the topography, but the 4th order stream, shown in a red colour on the map

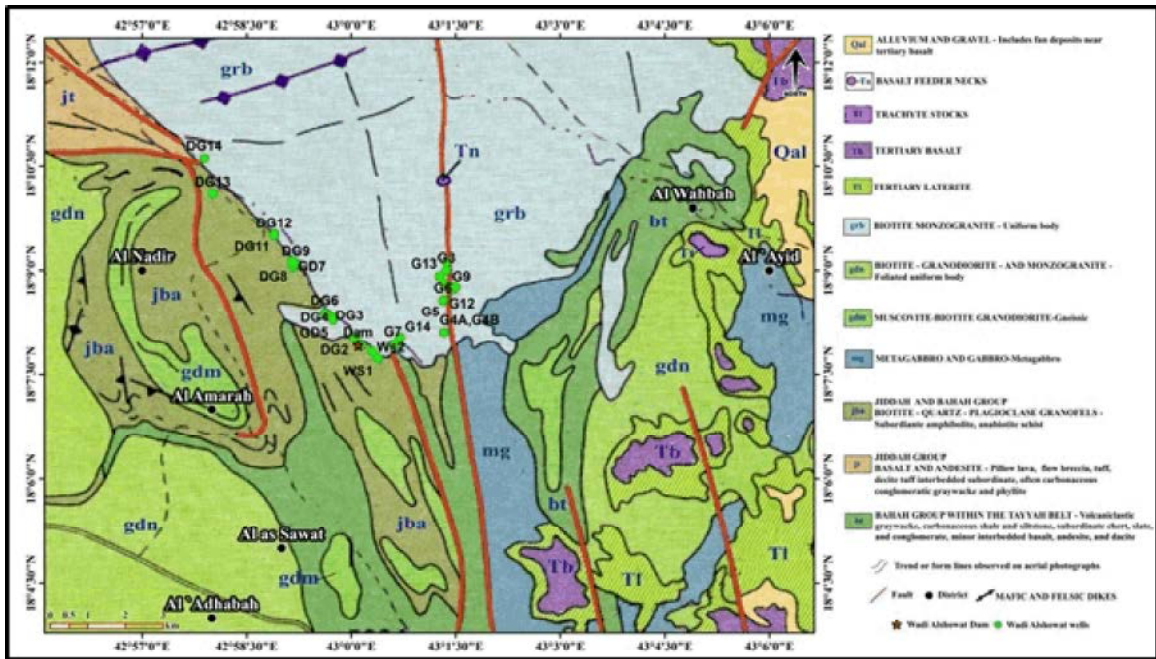


Fig. 4: Geologic map of Wadi Al-Shawat area



Fig. 5: Field photos showing fractures in the granitic rocks in Wadi Al-Shawat area

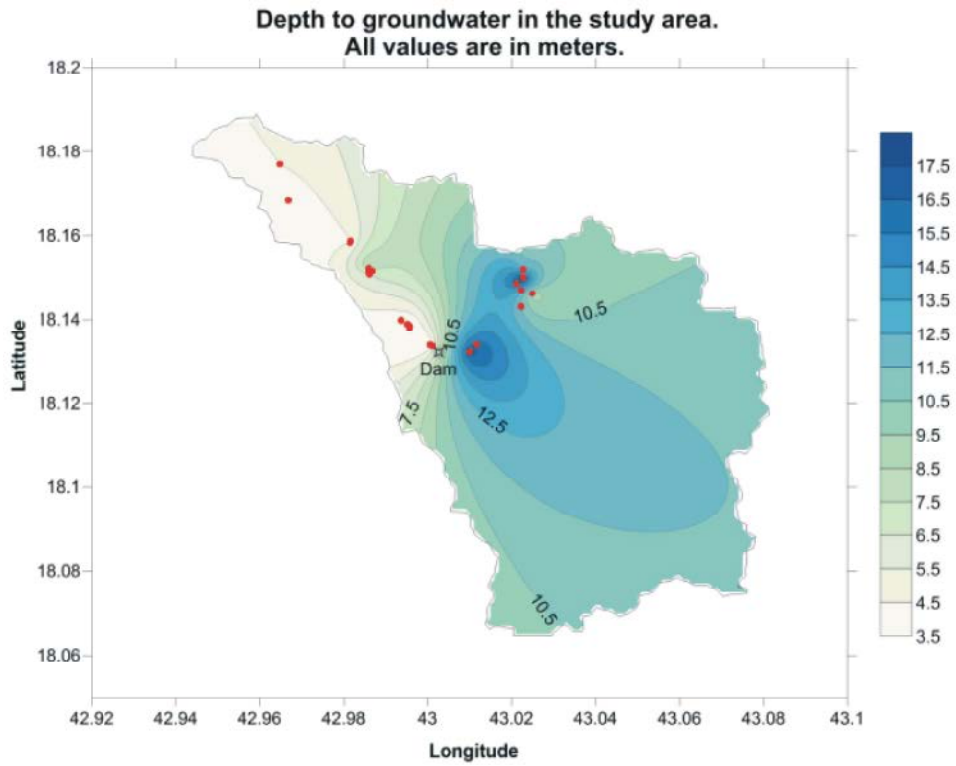


Fig. 6: The piezometric level in the study area (in meters above mean sea level)

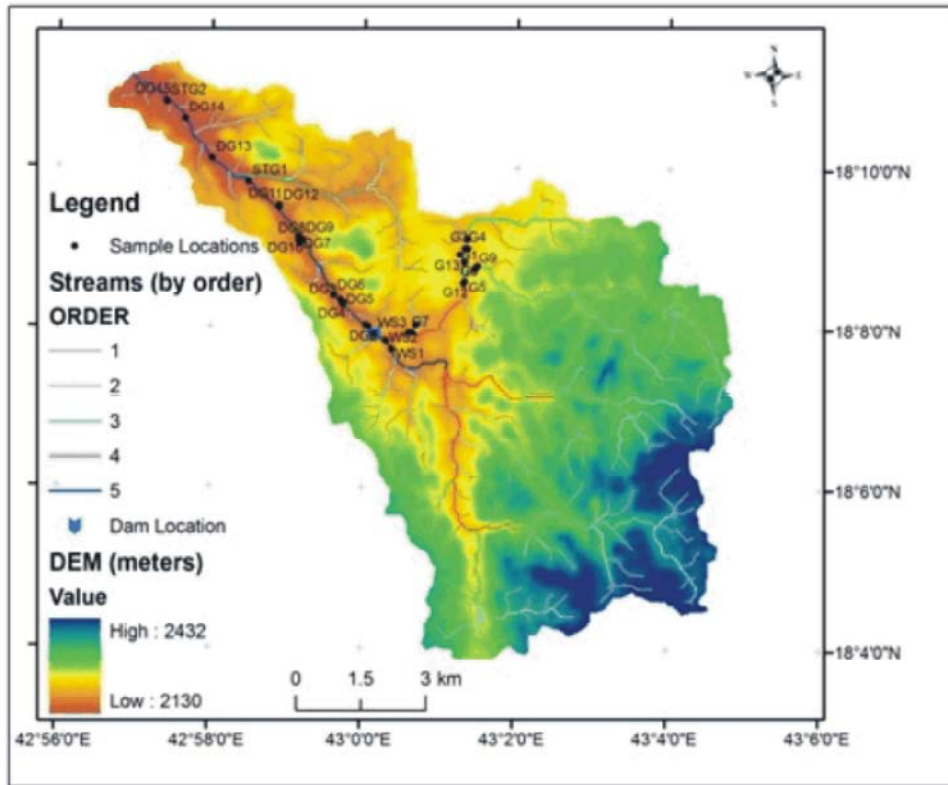


Fig. 7: Map showing the DEM of the study area, the dam location, streams and groundwater sample locations

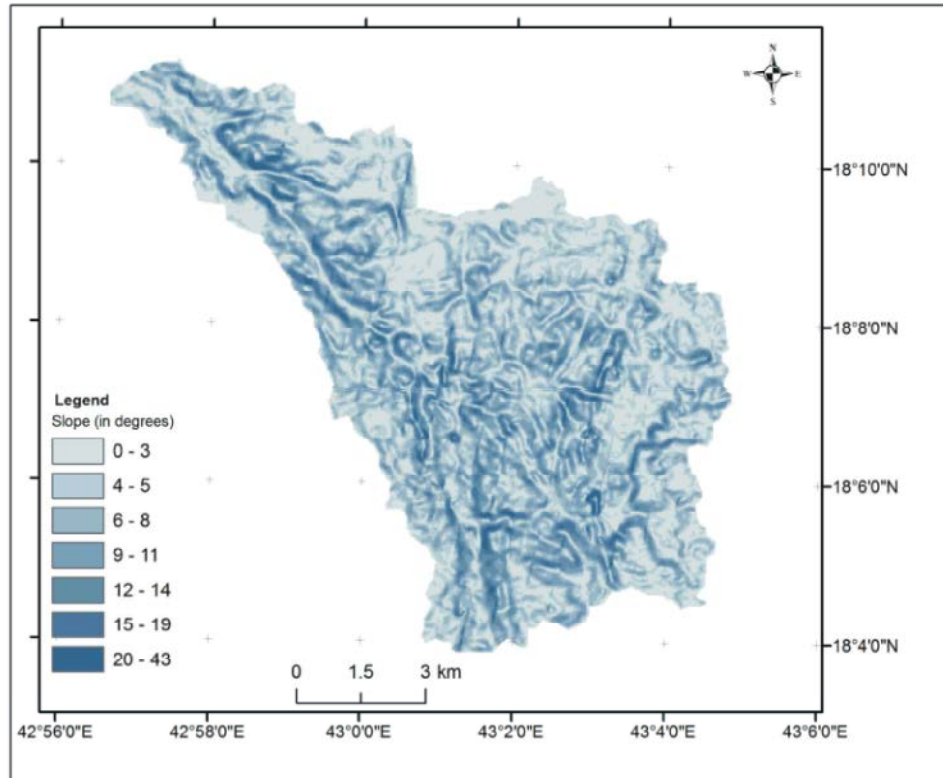


Fig. 8: The slope of the study area (in degrees)

and flowing in asouth to north direction, is structurally controlled and is influenced by a north-south trending lineament. The sample locations which lie on the streams other than 5th order stream in the north-central portion of the study area fall within this lineament zone. This lineament zone is the northward extension which controls the flow of the fourth order stream mentioned above. The average slope of the basin (Figure 8) is about 6.22°.

To understand the nature of the underlying geological formation, the drainage density (Dd) of the basin was calculated. Drainage density indicates the extent to which a landscape is dissected by streams, thus reflecting the tendency of the drainage basin to generate surface runoff, as well as the erodibility of the surface materials. Dd is defined as the ratio of the total length of the streams of all orders in a given basin to the total area of the basin and is expressed as km/km². A number of factors control the spatial and temporal evolution of Dd, including T the sub-surface geology [17], climate [18] and topographic relief and slope [19, 20, 21], Dd is also inversely related to the hydraulic conductivity of the underlying soil. Generally a high drainage density indicates resistant sub-surface material resulting in greater runoff during rainfall events.

The total stream length in the present study is 199.13 km. The basin is covered by basement rocks (igneous and metamorphosed igneous rocks) and there are practically no variations in the spatial distribution of the rainfall. In such conditions the drainage density of the basin should be high; but in factit is 2.144 km/km² which is characteristic of a coarse drainage. Field investigations have shown that the area is highly fractured/jointed and these fractures provide preferred pathways for the rainwater (which is the only source of groundwater recharge in the area) to percolate underground. The highly fractured nature of the bedrock in the area thus explains the low drainage density values.

The drainage texture, which refers to the spacing between the drainage lines, is a product of the drainage density and stream frequency. The stream frequency is the total number of streams of different orders in the basin divided by the area of the basin [22]. The drainage texture is dependent on the lithology, infiltration capacity and the relief of the terrain [23]. The presence of basement rocks and high slope should have resulted in a fine drainage texture (greater than 10 in the study area) but it was found to be 7.20, which is a further indication of weathered or fractured basement rocks. Field investigations in the area

point more towards fractured basement rocks. The presence of fractured rocks greatly influences the groundwater recharge from precipitation.

MATERIALS AND METHODS

Twenty-seven water samples were collected from the available shallow-dug wells along the Wadi AlShowat. Samples were collected in polyethylene bottles of one-litre capacity (Figure 9). Prior to filling with sampled water, these bottles were rinsed to minimize the chance of any contamination. Preservation of the samples and the analytical techniques used were in accordance with the standard methods set out by the American Public Health Association. Unstable parameters, such as hydrogen ion concentration (pH), total dissolved solids (TDS) and electrical conductivity (EC) were determined at the sampling sites with the help of a pH-meter, a TDS-meter and a portable EC-meter, respectively (Hanna Instruments, Michigan, USA). The sodium (Na^+), potassium (K^+), magnesium (Mg^{2+}) and calcium (Ca^{2+}) ions were determined using atomic absorption spectrophotometer (AAS). Bicarbonate (HCO_3^-) and chloride (Cl^-) were analyzed by volumetric methods. Sulphate (SO_4^{2-}) was estimated by the colorimetric and turbidimetric methods. Nitrate (NO_3^-) was measured by ionic chromatography.

Hydrochemical classification and groundwater evolution are discussed using bivariate plots, a Piper plot and a Durov Plot. For drinking water quality assessment, the results are compared with the World Health Organization²⁴ standards.



Fig. 9: Groundwater Sampled Wadi Al-Showat shallow wells

RESULTS AND DISCUSSION

General Groundwater Chemistry: Table 1 shows the general statistics of the analysed physio-chemical parameters for the 27 groundwater samples and their comparison with drinking water guidelines. The pH values for the analysed samples ranged from 7.14 to 8.04, with an average value of 7.43 and are thus very mildly alkaline. The TDS values ranged from 357 mg/l to 1310 mg/l. Na was the most dominant cation, followed by Ca, Mg and K. SO_4 was the most dominant anion, followed by Cl and HCO_3 . NO_3 values ranged from 5 to 31 mg/l and was therefore not of major concern in the area. 33.33% of the samples had TDS values above the maximum desirable limit [24]. 37% of the samples had Ca values in excess of the maximum desirable limits, whereas 33.33% and 40.74% of the samples had Cl and SO_4 in excess of the maximum desirable limits for drinking water (Table 1) [24].

To understand the influence of evaporation on the groundwater chemistry a plot of EC versus Na/Cl was prepared (Figure 10a). If evaporation is the major process governing the groundwater chemistry of a given area, the EC versus Na/Cl plot should be a straight line, indicating that the Na/Cl ratio remains constant with increasing salinity [25]. In the present study, the Na/Cl ratio increases with decreasing EC, indicating that Na is removed or Cl is added to the groundwater system at higher EC values. Since the chemistry of groundwater is not affected by the evaporation process, reverse ion exchange may be one of the factors responsible for the dominance of Cl over Na in the study area, as shown later in the Durov plot. The increase in Cl concentration may also be due to the presence of sewage water [26] (as was observed during field investigations). The fractured nature of the bedrock may facilitate the percolation of this waste water to the groundwater table.

On the Cl versus Na plot the 1:1 equiline indicates the halite dissolution. In Figure 10b, the data points are arranged in two groups. The first group of samples falls along the halite dissolution line whereas the second group of samples are represented by high Cl values as compared to Na. The excess of Cl over Na could be due to the removal of Na from the groundwater system as a result of reverse ion exchange (Zaidi et al., 2015) or the addition of Cl from anthropogenic sources [26].

An effective method of Ca, Mg and Na participation in ion exchange reactions can be validated by the plot of $\text{Na}^+ + \text{Cl}^-$ versus $(\text{Ca}^{2+} + \text{Mg}^{2+}) - (\text{HCO}_3^- + \text{SO}_4^{2-})$. Base ion exchange reactions within the groundwater should exhibit a slope of -1.0 on the plot, with the trend line showing an

Table 1: Statistics of the analyzed physio-chemical parameters of the 27 groundwater samples and their comparison with WHO standards (2011) for drinking water quality

| Parameters | Minimum | Maximum | Average | Standard Deviation | Drinking Water Quality Maximum desirable Limits (WHO 2011) | Percentage of samples exceeding the WHO limits* |
|--------------------------------|---------|---------|---------|--------------------|--|---|
| pH | 7.14 | 8.04 | 7.43 | 0.18 | 7-8 | 0 (0) |
| EC ($\mu\text{S}/\text{cm}$) | 329.00 | 2122.00 | 841.52 | 473.31 | | |
| TDS (mg/L) | 357.00 | 1310.00 | 792.67 | 304.06 | 1000.00 | 33.33 (9) |
| Ca(mg/L) | 24.00 | 214.00 | 84.44 | 63.66 | | 37.03 (10) |
| Mg(mg/L) | 12.00 | 84.00 | 43.37 | 16.45 | | |
| Na(mg/L) | 66.00 | 143.00 | 108.22 | 25.57 | 200.00 | 0 (0) |
| K(mg/L) | 8.00 | 19.00 | 12.00 | 2.71 | | |
| HCO ₃ (mg/L) | 46.00 | 162.00 | 86.26 | 33.65 | | |
| Cl(mg/L) | 93.00 | 390.00 | 217.85 | 102.39 | 250.00 | 33.33 (9) |
| SO ₄ (mg/L) | 96.00 | 386.00 | 240.52 | 84.09 | 250.00 | 40.74 (11) |
| NO ₃ (mg/L) | 5.00 | 31.00 | 19.59 | 6.63 | 50 | 0 (0) |

* Number in parenthesis indicates the number of samples having values more than the maximum permissible limits.

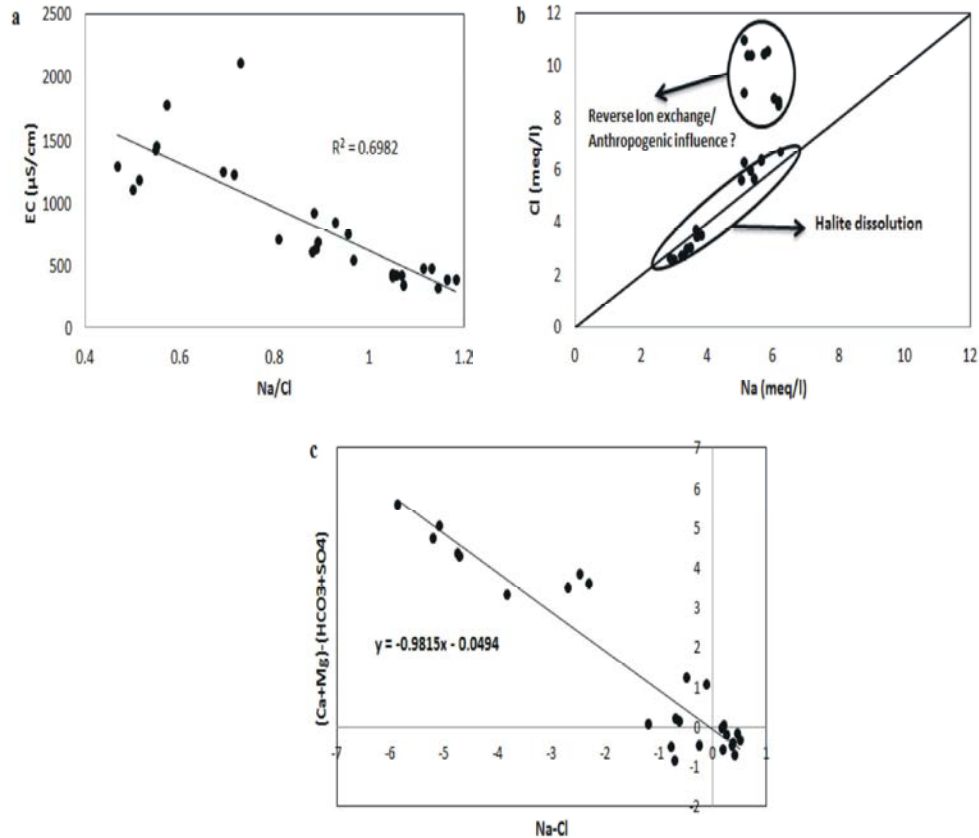


Fig. 10: EC versus Na/Cl plot to show the influence of evaporation on groundwater chemistry; b) Cl versus Na plot to show halite dissolution and the possible ion exchange/reverse ion exchange phenomenon; c) (Ca+Mg)-(HCO₃+SO₄) versus Na-Cl to assess the influence of base ion exchange reactions on groundwater chemistry

intercept close to 0 on the y axis [27, 28]. In the present case (Figure 10c) the slope is -0.98 (approximately -1) and the intercept is -0.049 (close to 0) and this should indicate that Ca, Mg and Na concentrations are interrelated through the ion exchange process. Closer examination of the plot,

however, shows that only a few samples fall along the trend line, with most falling above or below the line, indicating that the groundwater chemistry of those samples is not governed by the base ion reactions and thus pointing towards anthropogenic sources.

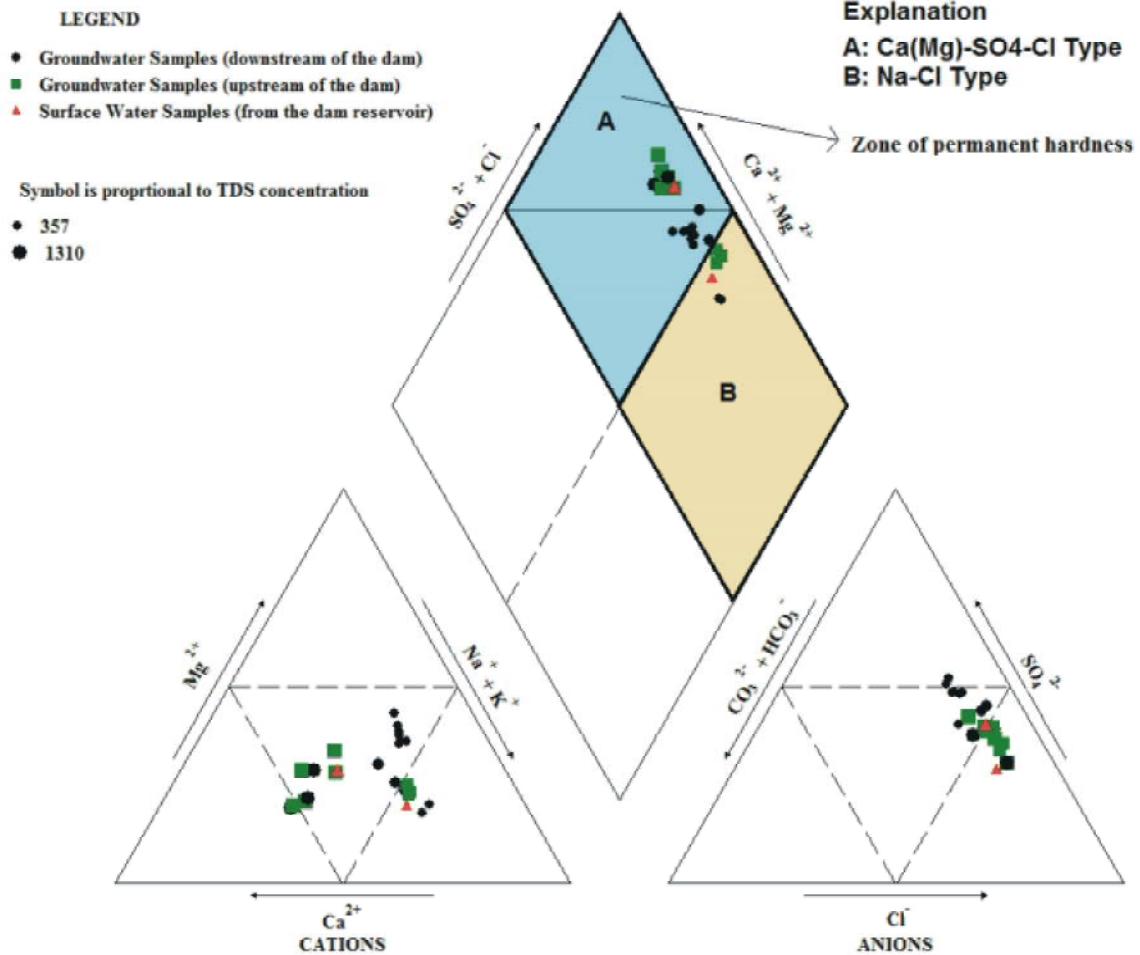


Fig. 11: Piper plot of the analyzed samples

Groundwater Classification

Piper Plot: The values of the major ions in the analysed water samples were plotted on a Piper trilinear diagram in order to understand the hydrochemical regime of the study area. The Piper trilinear diagram for the groundwater samples is presented in Figure 11 and clearly explains the variations in cation and anion concentrations in the study area.

The symbols on the Piper plot have been classified according to the type of sample. Black circles symbolise groundwater samples that have been collected downstream of the dam and comprise 17 samples. The green squares, meanwhile, represent the groundwater samples collected from upstream of the dam and include eight samples, whereas the red samples represent the two water samples collected from the dam reservoir itself.

The water in the study area belongs to the SO₄-Cl type. This type can be further subdivided into two types of groundwater facies depending on the abundance of the

cations. The first facies is the Ca(Mg)-SO₄-Cl type and comprises a total of 20 samples (five upstream, one surface water sample and 14 samples from the downstream direction). This groundwater facies also contains samples which have undergone reverse ion exchange whereby the Na in the groundwater has been replaced by Ca and Mg in the aquifer material. As shown in the map, some of these water samples are also characterized by permanent hardness due to the formation of non-carbonate salts, mostly among the samples from upstream of the dam.

The second groundwater facies belong to the Na-Cl type and is represented by simple halite dissolution and includes a total of six water samples (three samples from upstream, one surface water sample and two samples from the downstream direction). In general, the samples belonging to the Ca(Mg)-SO₄-Cl type are characterized by high TDS values. Most of the samples from the upstream side of the dam, one surface water sample and one sample in the downstream direction just next to the dam reservoir

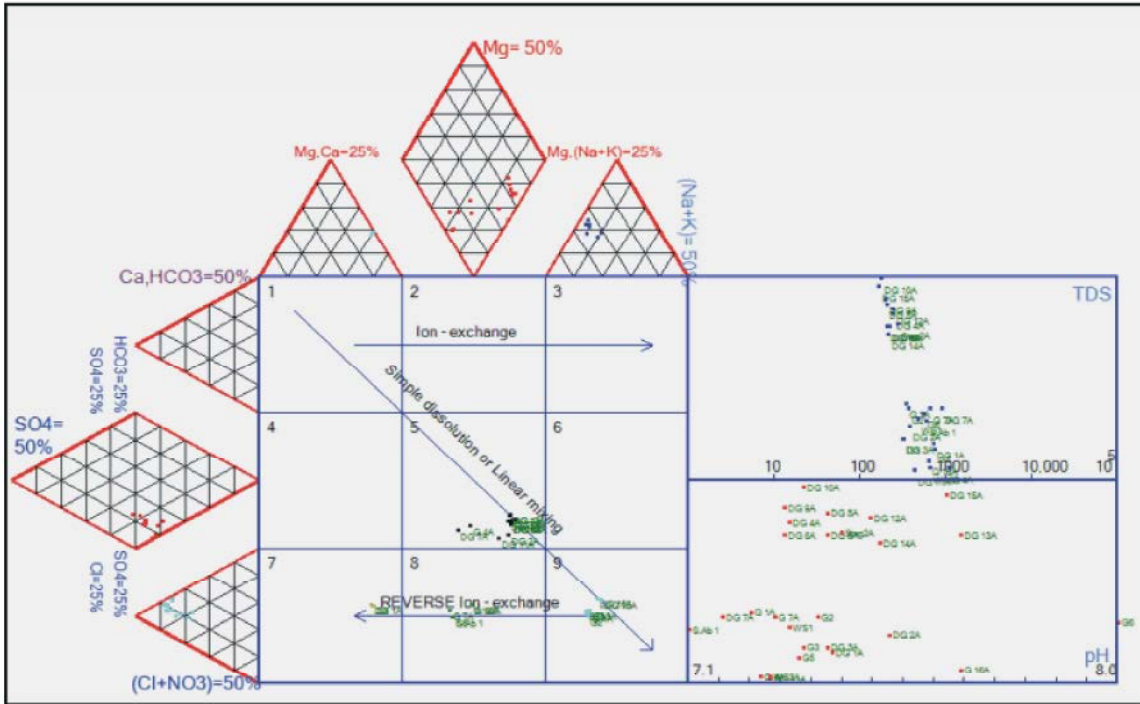


Fig. 12: Durov plot of the analyzed samples

are characterized by high TDS values. The samples farther away in the downstream side of the dam show lower TDS values. This may be the result of the dilution of groundwater in the downstream side due to water percolation from the dam reservoir.

Durov Plot: The processes responsible for the chemical evolution of groundwater in a given hydrological setup are better explained by the expanded Durov diagram [29]. The DurovPwin software [30] was used to prepare the Durov plot (Figure 12). On the Durov plot the samples fall into the Type 5, Type 7, Type 8 and Type 9 categories. The highest number of samples falls within the Type 5 category, which represents the mixed type of groundwater facies, although they are closer to the Type 8 and Type 9 classes which are characterized by the dominance of SO_4 and Cl. The type 7 groundwater facies represents the Ca- Cl_2 type of groundwater. This is a very rare type of groundwater facies and is characterized by the abundance of Ca over Na and Cl over SO_4 . This particular type of groundwater facies falls within the zone of permanent hardness on the piper plot.

The type 8 facies is represented by water which is characterized by reverse ion exchange or the abundance of Ca+Mg over Na. The type 9 facies is represented by simple halite dissolution as represented by the Na-Cl water type on the Piper plot.

CONCLUSIONS

The main aim of the present study was to evaluate and assess the shallow groundwater aquifer along Wadi Al Showat, in the Khamis Mushayt District of south-west Saudi Arabia using hydrochemical and geological analysis. The field investigation indicated that the basement rocks in the area are dissected by two main sets of fractures that are oriented in the west to -north-west and east to west directions. These fracture systems serve as the main aquifer in the area and are important from the hydrogeological point of view since they allow the aquifer to perform a storage and transmissive function. At the same time the fracture aquifer system makes it highly vulnerable to pollution from domestic and agricultural activities.

Ion exchange, halite dissolution, reverse-ion exchange and some impact from anthropogenic activities are responsible for the present groundwater chemistry in the area. Fortunately, the hydrochemical analysis indicates that the agricultural and domestic activities along the wadi currently have only a limited adverse impact on the groundwater quality in the area. Bearing in mind a) the fractured nature of the aquifer b) the shallow depth to the groundwater table and c) the increasing level of domestic and agricultural activities, it is important, however, to maintain periodic groundwater

quality monitoring in order to assess the influence of anthropogenic activities on the groundwater regime. Some regulatory framework for groundwater pumping, domestic sewage waste disposal and agricultural activities should also be put in place by the concerned authorities in the area to prevent depletion and pollution of the groundwater.

ACKNOWLEDGEMENTS

The authors extend their appreciation to the Deanship of Scientific Research at King Saud University for funding this work through research group (Prolific Research Group (PRG-1436-21)).

REFERENCES

1. Al Alawi, J. and M. Abdulrazzak, 1996. Water in the Arabian Peninsula: problems and perspectives. In: Rogers, P., Lydon, P. (Eds.), *Water in the Arab World: Perspectives and Prognoses*. The American university in Cairo press, Egypt, pp: 171-202.
2. Al Ammar, A.I. and S.E. Kruse, 2016. Resistivity soundings and VLF profiles for siting groundwater wells in a fractured basement aquifer in the Arabian Shield, Saudi Arabia. *Journal of African Earth Sciences*, 116: 56-67.
3. Davis, S.N. and L.J. Turk, 1964. Optimum depth of wells in crystalline rocks, *Ground Water*, 2: 6-11.
4. Houston, J.T. and R.T. Lewis, 1988. The Victoria Province drought relief project, II. Borehole yield relationships, *Ground Water*, 26: 418-426.
5. Acworth, R.I., 1987. The development of crystalline basement aquifers in a tropical environment, *Q. J. Eng. Geol.*, 20: 265-272.
6. Wright, E.P., 1992. The hydrogeology of crystalline basement aquifers in Africa. *Geol. Soc. London Spec. Publ.*, 66: 1-27.
7. Taylor, R. and K. Howard, 2000. A tectono-geomorphic model of the hydrogeology of deeply weathered crystalline rock: evidence from Uganda. *Hydrogeology Journal*, 8(3): 279-94.
8. Wyns, R., J.M. Baltassat, P. Lachassagne, A. Legchenko, J. Vairon and F. Mathieu, 2004. Application of SNMR soundings for groundwater reserves mapping in weathered basement rocks (Brittany, France), *Bull. Soc. Geol. Fr.*, 175(1): 21-34.
9. Dewandel, B., P. Lachassagne, R. Wyns, J.C. Maréchal, N.S. Krishnamurthy, 2006. A generalized 3-D geological and hydrogeological conceptual model of granite aquifers controlled by single or multiphase weathering. *Journal of Hydrology*, 330(1): 260-84.
10. Cook, P.G., 2003. A guide to regional groundwater flow in fractured rock aquifers (pp: 107). Australia: CSIRO.
11. Singhal, B. and R. Gupta, 1999. *Applied Hydrogeology of Fractured Rocks*. Springer, 1999, ISBN: 978-94-015-9210-9 (Print) 978-94-015-9208-6 (Online).
12. Gustafson, G.U. and J. Krásni, 1994. Crystalline rock aquifers: their occurrence, use and importance. *Applied Hydrogeology*, 2(2): 64-75.
13. Subyani, A.M., A.A. Al-Modayan and F.S. Al-Ahmadi, 2010. Topography, seasonal and aridity influences on rainfall variability in western Saudi Arabia. *Journal of Environmental Hydrology*, 18(2): 11.
14. World Bank group, Climate change knowledge portal for development practitioners and policy makers (<http://sdwebx.worldbank.org/climateportal/>), 2016.
15. Greenwood, W.R., 1985. Explanatory notes to the geologic map of the Abha quadrangle, sheet 18F, Kingdom of Saudi Arabia.
16. Hempton, M.R., 1987. Constraints on Arabian plate motion and extensional history of the Red Sea. *Tectonics*, 6(6): 687-705.
17. Kelson, K. and S. Wells, 1989. Geologic influences on fluvial hydrology and bedload transport in small mountainous watersheds, northern New Mexico, USA. *Earth Surf Process Landforms*, 14(8): 671-90.
18. Gregory, K. and V. Gardiner, 1975. Drainage density and climate. *Geomorphol.*, 19(3): 287-98.
19. Montgomery, D. and W. Dietrich, 1989. Source areas, drainage density and channel initiation. *Water Resources Research*, 25(8): 1907-18.
20. Oguchi, T., 1997. Drainage density and relative relief in humid steep mountains with frequent slope failure. *Earth Surf Proc Land.*, 22: 107-20.
21. Schumm, S., 1956. The role of creep and rain-wash on the retreat of badland slopes South Dakota. *Am. J. Sci.*, 254(11): 693-706.
22. Horton, R.E., 1945. Erosional development of streams and their drainage basins; hydrophysical approach to quantitative morphology. *Geol. Soc. Am. Bull.*, 56: 275-370.

23. Zaidi, F.K. and M. Mukhopadhyay, 2015. Morphometric analysis of the Scoria Cones and drainage pattern for the Quaternary and older Volcanic Fields in parts of the Large Igneous Province (LIP), Saudi Arabia. *Journal of African Earth Sciences*, 110: 1-13.
24. WHO, 2011. Guidelines for drinking-water quality. World Health Organization, 216: 303-4.
25. Jankowski, J. and R.I. Acworth, 1997. Impact of Debris-Flow Deposits on Hydrogeochemical Processes and the Development of Dryland Salinity in the Yass River Catchment, New South Wales, Australia. *Hydrogeology Journal*, 5(4): 71-88.
26. Mondal, N.C., V.K. Saxena and V.S. Singh, 2005. Assessment of groundwater pollution due to tannery industries in and around Dindigul, Tamilnadu, India. *Environmental Geology*, 48: 149-157.
27. Fisher, R.S. and W.F. Mullican, 1997. Hydrochemical evolution of sodium-sulphate and sodium-chloride groundwater beneath the northern Chihuahuan Desert, Trans-Pecos, Texas, USA. *Hydrogeology Journal*, 5: 4-16.
28. Rajmohan, N. and L. Elango, 2004. Identification and evolution of hydrogeochemical processes in the groundwater environment in an area of the Palar and Cheyyar River Basins, Southern India. *Environmental Geology*, 46(1): 47-61.
29. Lloyd, J.W. and J.A. Heathcote, 1985. Natural inorganic hydrochemistry in relation to groundwater: an introduction. Clarendon Press, Oxford, pp: 294.
30. Al-Bassam, A.M. and A.R. Khalil, 2012. DurovPwin: a new version to plot the expanded Durov diagram for hydro-chemical data analysis. *Comput Geosci.*, 42: 1-6.